physchem

MDPI

Communication

Scalable Synthesis of 2D TiNCl via Flash Joule Heating

Gabriel A. Silvestrin [1], Marco Andreoli [1], Edson P. Soares [1], Elita F. Urano de Carvalho [1], Almir Oliveira Neto [1] and Rodrigo Fernando Brambilla de Souza [1,2,*]

[1] Instituto de Pesquisas Energéticas e Nucleares, IPEN-CNEN/SP, Cidade Universitária, Av. Professor Lineu Prestes, 2242, São Paulo 05508-900, SP, Brazil
[2] Comissão Nacional de Energia Nuclear, CNEN, Rio de Janeiro 22294-900, RJ, Brazil
* Correspondence: souza.rfb@gmail.com

Abstract

A scalable synthesis of two-dimensional titanium nitride chloride (TiNCl) via flash Joule heating (FJH) using titanium tetrachloride ($TiCl_4$) precursor has been developed. This single-step method overcomes traditional synthesis challenges, including high energy consumption, multi-step procedures, and hazardous reagent requirements. The structural and chemical properties of the synthesized TiNCl were characterized through multiple analytical techniques. X-ray diffraction (XRD) patterns confirmed the presence of TiNCl phase, while Raman spectroscopy data showed no detectable oxide impurities. Fourier transform infrared spectroscopy (FTIR) analysis revealed characteristic Ti–N stretching vibrations, further confirming successful titanium nitride synthesis. Transmission electron microscopy (TEM) imaging revealed thin, plate-like nanostructures with high electron transparency. These analyses confirmed the formation of highly crystalline TiNCl flakes with nanoscale dimensions and minimal structural defects. The material exhibits excellent structural integrity and phase purity, demonstrating potential for applications in photocatalysis, electronics, and energy storage. This work establishes FJH as a sustainable and scalable approach for producing MXenes with controlled properties, facilitating their integration into emerging technologies. Unlike conventional methods, FJH enables rapid, energy-efficient synthesis while maintaining material quality, providing a viable route for industrial-scale production of two-dimensional materials.

Keywords: MXenes; TiNCl; flash Joule heating method; 2D material

Academic Editor: Michael Lyons

Received: 19 May 2025
Revised: 2 July 2025
Accepted: 25 July 2025
Published: 28 July 2025

Citation: Silvestrin, G.A.; Andreoli, M.; Soares, E.P.; de Carvalho, E.F.U.; Neto, A.O.; de Souza, R.F.B. Scalable Synthesis of 2D TiNCl via Flash Joule Heating. *Physchem* **2025**, *5*, 30. https://doi.org/10.3390/physchem5030030

1. Introduction

MXenes represent a relatively new class of two-dimensional (2D) materials, composed primarily of transition metal carbides, nitrides, and carbonitrides. These materials are derived from their corresponding MAX phase precursors, where M represents an early transition metal, A is typically an element from groups 13–16 (such as aluminum or silicon), and X refers to carbon or nitrogen. The removal of the A-layer through selective etching results in the formation of layered MXene structures, which exhibit a wide range of tunable physicochemical properties [1]. Their structural configuration and surface chemistry have driven extensive research interest across multiple technological domains [2,3].

The characteristic sheet-like morphology of MXenes endows them with several advantageous features. Among these are high electrical conductivity, which is comparable to that of metals, a large surface area that facilitates interaction with surrounding environments, and notable mechanical flexibility that allows integration into flexible devices [4]. Additionally, MXenes demonstrate good thermal stability and can be easily modified through

surface functionalization, further enhancing their applicability in various fields such as energy storage, electrochemical sensing, electromagnetic interference shielding, water purification, catalysis, and biomedical engineering [1]. Their versatility is largely attributed not only to their intrinsic physical and electronic properties but also to the ability to tailor their chemical composition and surface terminations.

Several synthetic routes have been developed for the production of MXenes, each presenting specific advantages and limitations in terms of process control, product quality, and scalability. One of the most widely adopted methods is acid etching, wherein fluoride-containing solutions are used to selectively remove the A-element from the MAX phase precursor. This approach enables the intercalation and exfoliation of individual MXene layers, resulting in a 2D structure with exposed surfaces that can be further functionalized [5]. While effective, this method often involves the use of corrosive chemicals and requires careful handling due to safety concerns.

An alternative technique known as molten salt etching has been proposed as a less hazardous option. In this process, fluoride salts in a molten state replace aqueous etchants, potentially reducing environmental impact. However, this method still demands high temperatures and specialized equipment, limiting its practicality for large-scale production [6].

Layered MNX compounds (metal–nitrogen–halide systems), which belong to the same structural class but do not require alloy formation for exfoliation, can be synthesized chemically. For instance, a closed-system synthesis route for TiNCl using sodium amide ($NaNH_2$) as a nitrogen source yields highly crystalline samples through thermal decomposition of aminated titanium chloride [7], a hydrothermal method applied to obtain Ti 2D advanced materials, as an MNX [3]. On the other hand, chemical vapor deposition (CVD) offers a bottom-up synthesis strategy, allowing precise control over the composition and morphology of MXene structures. Although CVD based approaches [8,9] provide superior material quality, they are generally more complex and costly, making them less suitable for industrial-scale manufacturing.

Among the various MXene compositions, titanium-based systems—particularly titanium carbide ($Ti_3C_2T_x$) and titanium nitride (TiN)—have received significant research interest due to their favorable combination of electrical, mechanical, and chemical properties. Titanium nitride, in particular, exhibits high thermal stability, excellent corrosion resistance, and a metallic conductivity profile, making it a promising candidate for applications in energy conversion and storage, plasmonics, and electronic devices [4]. Recent studies have explored the possibility of modifying TiN by introducing halogen atoms into its crystal lattice, aiming to adjust its electronic and optical characteristics. Halogenation has been shown to effectively modulate the band structure of TiN, thereby expanding its utility in optoelectronic and photocatalytic applications.

For instance, experimental investigations have demonstrated that halogenated TiN monolayers, such as TiNCl and TiNBr, exhibit modified electronic structures with widened optical bandgaps—up to approximately 1.85 eV. This change in the bandgap is particularly relevant for applications like photocatalytic water splitting, where the ability to absorb visible light and efficiently separate charge carriers plays a critical role in overall performance [10]. Despite these promising findings, the synthesis of halogenated titanium nitride compounds remains challenging. Conventional methods often require multi-step processes, involve the use of toxic reagents, and consume substantial amounts of energy, which hamper their feasibility for scalable production.

Therefore, there is a growing need to develop more efficient, cost-effective, and environmentally benign synthetic strategies for producing halogenated MXenes such as TiNCl [11]. Addressing these challenges is essential to enable the broader adoption of

such materials in practical applications ranging from renewable energy technologies to next-generation electronic devices.

One emerging technique that shows promise in this context is flash Joule heating (FJH). This method has gained attention for its simplicity, rapid processing time, and compatibility with a variety of precursor materials. FJH involves applying a short, high-intensity electric current pulse through a solid-state precursor, generating localized temperatures that can exceed several thousand degrees Celsius within milliseconds. This extreme thermal environment facilitates the decomposition and vaporization of the precursor, followed by rapid quenching and condensation to form nanoscale particles or thin films under controlled conditions [12,13]. In the present study, we investigate the synthesis of TiNCl using $TiCl_4$ as a precursor in a flash Joule heating setup. The objective is to evaluate the viability of this approach as an alternative to conventional synthesis methods, with a focus on achieving high-quality nanomaterials in a single step. By leveraging the rapid and energy-efficient nature of FJH, we aim to overcome some of the limitations associated with existing techniques, including long reaction times, harsh chemical treatments, and high energy consumption.

2. Materials and Methods

Titanium tetrachloride ($TiCl_4$, Sigma-Aldrich, 99.99% purity) was carefully introduced into a high-purity graphite crucible with an internal volume of 2.5 mL. The crucible was cleaned using analytical-grade acetone to remove organic residues and then dried under continuous dry nitrogen gas flow. Once introduced into the crucible, the titanium tetrachloride was allowed to solidify under a highly controlled inert nitrogen (N_2) atmosphere. The nitrogen atmosphere was maintained at atmosphere pressure and the system temperature was carefully regulated at -25 °C using a closed-loop cryogenic refrigeration system. This low-temperature environment was selected to promote uniform freezing of the precursor, ensuring that no local melting or partial decomposition would occur. The nitrogen atmosphere was continuously flushed to prevent the ingress of trace amounts of oxygen (which can produce TiO_2 and/or oxychlorides) or ambient moisture, both of which could lead to undesirable side reactions or partial hydrolysis of the titanium tetrachloride. The use of an inert nitrogen blanket not only suppresses the introduction of impurities but also plays a pivotal role as a nitrogen source for the TiNCl structure.

After the solidification step, the crucible was closed and maintained in the nitrogen atmosphere inert conditions and was then subjected to a precisely programmed series of electrical discharge treatments. In total, 200 individual discharge cycles were executed, with each cycle delivering an energy input of 100 coulombs at an operating voltage of 65 V. The entire sequence of electrical discharges was completed within an intense interval of three minutes. Following this treatment, the processed material was recovered from the crucible.

Structural characterization of the treated material was primarily carried out using X-ray diffraction (XRD) analysis. The XRD measurements were performed with a Rigaku Miniflex II diffractometer equipped with a copper Kα radiation source (wavelength $\lambda = 1.54056$ Å). Data acquisition was conducted across a broad 2θ angular range spanning from 5° to 65°, employing a fine step size of 0.02° and an integration time of 2.0 s per step. These parameters ensured high-resolution diffraction patterns capable of revealing subtle changes in crystallinity, phase composition, and possible emergence of new crystalline phases that may have formed during discharge treatment.

Raman spectroscopy was employed to probe the vibrational properties and chemical bonding within the processed material. The Raman spectra were acquired using a Horiba Scientific MacroRam Raman spectrometer with a laser excitation wavelength of 785 nm.

This specific wavelength was carefully selected to minimize fluorescence background, which is particularly advantageous when analyzing titanium compounds and any residual carbonaceous species originating from the graphite crucible. The Raman measurements were conducted in a backscattering configuration, with each scan having an acquisition time of 30 s. Multiple accumulations were averaged to enhance the overall signal-to-noise ratio.

To further elucidate the surface chemistry and identify functional groups present on the treated material, diffuse reflectance infrared Fourier transform (DRIFT) spectroscopy was conducted. This analysis was performed using a Nicolet® 6700 FT-IR spectrometer equipped with a Pike® diffuse reflectance accessory and a highly sensitive, liquid nitrogen-cooled MCT detector. The DRIFT method is particularly well-suited for analyzing finely divided powders or nanoparticulate samples. Infrared spectra were collected with a spectral resolution of 4 cm^{-1} and 128 scans.

In addition to spectroscopic analyses, the microstructural features and particle size distribution of the synthesized material were investigated using transmission electron microscopy (TEM). TEM imaging was carried out on a JEOL JEM-2100 electron microscope operated at an accelerating voltage of 200 kV. Prior to TEM observation, the samples were ultrasonically dispersed in high-purity ethanol for approximately 15 min to effectively break up any agglomerates and to ensure a representative dispersion of individual particles. A small drop of the resulting dispersion was then deposited onto a carbon-coated copper grid and subsequently dried under vacuum conditions to prevent the adsorption of atmospheric moisture. Furthermore, selected area electron diffraction (SAED) patterns were collected to provide complementary local crystallographic information, supporting the phase identification performed by XRD.

3. Results and Discussion

The XRD pattern of the synthesized material, shown in Figure 1a, reveals broad, diffuse scattering features with a dominant intensity maximum centered at approximately $2\theta \approx 22.5^\circ$. This characteristic profile is indicative of an amorphous or poorly ordered phase, where long-range crystallographic periodicity is either absent or significantly disrupted. The presence of this diffuse halo suggests that the material possesses a predominantly amorphous character at the atomic scale, likely resulting from rapid quenching or non-equilibrium synthesis conditions [14]. Superimposed on this amorphous background, several sharp Bragg reflections are observed at $2\theta \approx 11^\circ$, 26°, 36°, 38°, 43°, 45°, 46°, 51°, 53°, and 60°, which correspond to the (001), (101), (012), (111), (112), (013), (200), (113), (104), and (114) planes, respectively, of titanium nitride chloride (TiNCl), as a JCPDS card #18-1399. The coexistence of these well-defined crystalline peaks within the amorphous matrix confirms the presence of nanocrystalline domains embedded in a disordered phase, indicating a composite microstructure composed of both ordered and disordered regions. Such dual-phase systems are often associated with enhanced functional properties, including improved mechanical strength and tailored electrical conductivity, due to the synergistic effects between crystalline and amorphous domains.

Furthermore, a systematic shift of the diffraction peaks toward higher 2θ angles is observed relative to the standard TiNCl reference. This shift indicates a reduction in interplanar d-spacing, which may arise from residual internal strain, lattice contraction, or possible incorporation of defects and vacancies during synthesis. These effects can be attributed to compositional inhomogeneity, rapid thermal transformation caused by the flash Joule heating process, or nanoscale confinement due to rapid reduction during electrical discharge [15], all of which are known to influence the structural parameters of transition metal nitrides. Such lattice distortions are often correlated with unique physical properties, including modified electronic band structures [16].

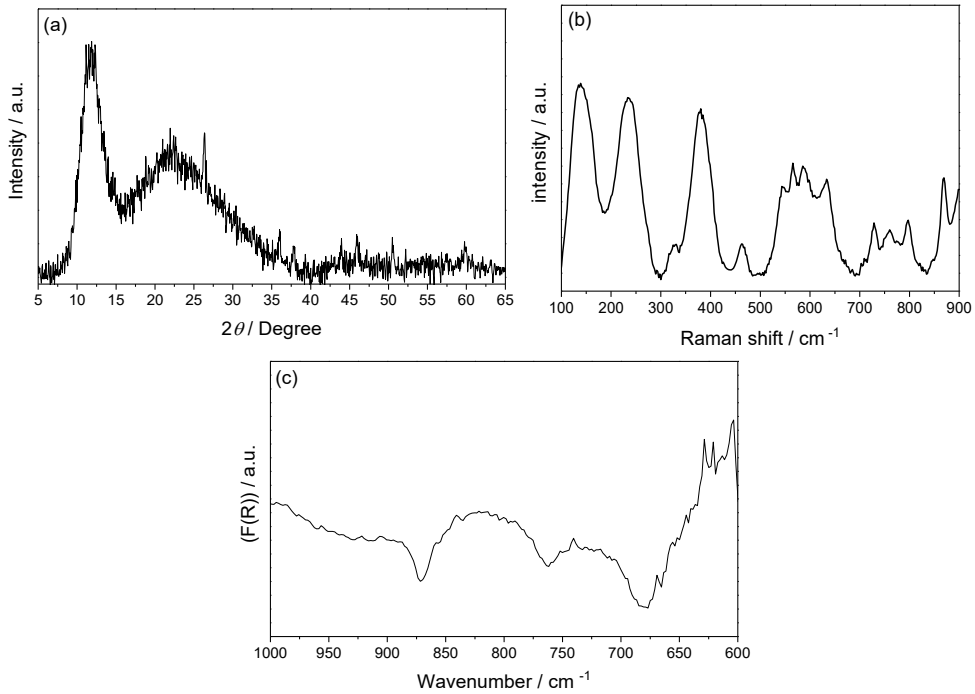

Figure 1. (**a**) XRD pattern, (**b**) Raman spectrum, and (**c**) DRIFT spectrum of titanium nitride synthesized via the flash Joule heating method.

The Raman spectrum of the synthesized material (Figure 1b) provides further evidence for the formation of titanium nitride (TiN). Distinct vibrational features are observed across the spectral range. Low-frequency bands at approximately 138, 231, 315, and 460 cm^{-1} correspond to acoustic phonon modes, consistent with reported values for TiN, and are attributed to collective lattice vibrations involving both Ti and N atoms [17,18]. In addition, optical phonon modes at 568 and 638 cm^{-1} are characteristic of stoichiometric TiN and are associated with intra-unit-cell displacements [18,19]. The presence of a notable high-frequency feature at ~845 cm^{-1}, assigned to a combined acoustic–optical (A+O) mode [20], further distinguishes the vibrational profile. This hybrid mode, rarely observed in ideal crystalline materials, indicates a breakdown of conventional Raman selection rules, likely due to structural disorder or the presence of lattice imperfections such as vacancies, dislocations, or grain boundaries, as proposed by Judek et al. [21]. These defects are consistent with the synthesis conditions employed and may significantly influence the material's electronic and thermal transport properties.

Additional peaks at 378 and 548 cm^{-1}, as reported by Urbankowski et al. [5], are attributed to out-of-plane A_1g symmetry modes involving coordinated Ti–N vibrations. Their presence corroborates the identification of the material as titanium nitride and provides insight into its local structural arrangement, suggesting the retention of key vibrational characteristics despite the presence of disorder. Notably, no vibrational signatures associated with titanium dioxide (TiO_2) were detected. The absence of characteristic anatase bands (165, 201, 396, 504, 621 cm^{-1}) and rutile peaks (148, 518 cm^{-1}) [19] confirms that the product is free from detectable oxide phases. This phase purity is crucial, as even trace levels of TiO_2 can degrade the electronic conductivity and chemical stability of TiN, thereby limiting its performance in electronic and catalytic applications. The absence of oxide-related bands supports the material's structural and compositional integrity, which is essential for high-performance applications.

Complementary information regarding the chemical composition and bonding configuration was obtained through DRIFTS, as shown in Figure 1c. The spectrum displays several prominent absorption bands that are consistent with Ti–N vibrational stretching modes.

Specifically, absorptions were observed at approximately 605 cm^{-1} [22], 740 cm^{-1} [23], and 905 cm^{-1} [17], all of which align well with literature values for stoichiometric TiN. These infrared-active modes provide further evidence of the successful formation of the nitride compound and support the conclusions drawn from both XRD and Raman analyses. The combination of these complementary techniques not only confirms the phase purity and structural integrity of the synthesized TiN but also highlights the effectiveness of the flash Joule heating method in producing high-quality nitride materials with tailored structural features.

To gain deeper insights into the microstructural characteristics of the synthesized material, representative TEM images, shown in Figure 2a,b, reveal the presence of thin, plate-like structures with high electron transparency under a 200 kV accelerating voltage. This observation indicates that the material possesses a lamellar morphology with a thickness on the nanometer scale, which is consistent with the formation of two-dimensional nanostructures. Such morphology is often associated with improved stability during electron microscopy, as the reduced thickness minimizes beam-induced artifacts and allows for more reliable imaging.

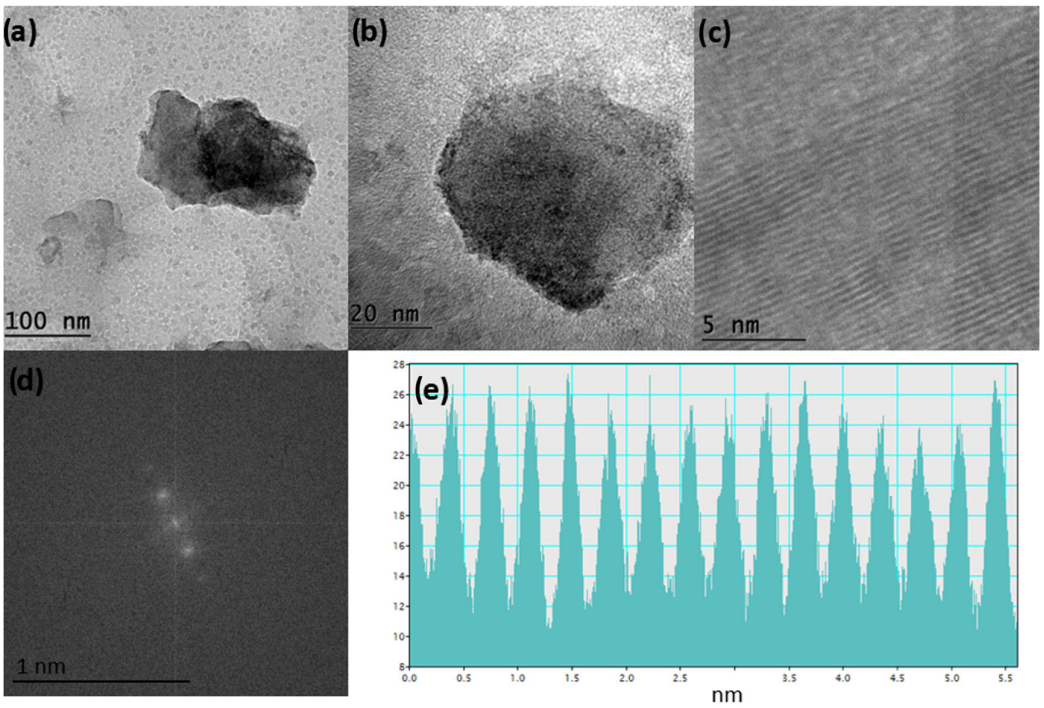

Figure 2. (**a**–**c**) TEM micrographs of TiNCl at different magnifications; (**d**) fast Fourier transform diffraction pattern obtained from the region highlighted in (**c**); and (**e**) intensity profile of lattice fringes extracted from image (**c**).

Notably, the synthesized samples exhibited remarkable resistance to beam damage and structural degradation, even under prolonged exposure to the electron beam. This robust behavior suggests that the material possesses a high degree of structural integrity and is less susceptible to radiation-induced amorphization compared to many other nanoscale systems. In certain regions, overlapping layers of these lamellae were observed, a feature that is commonly associated with the self-assembly of nanosheets during synthesis or subsequent cooling processes. This stacking behavior, as previously reported by Djire et al. for analogous 2D nanostructures [17], can significantly influence the material's transport and mechanical properties by altering the interlayer interactions and charge carrier pathways.

HRTEM imaging, presented in Figure 2c, further elucidates the structural order within specific domains of the material. Well-resolved lattice fringes are visible, indicating a high degree of crystallinity in these regions. The measured spacing between adjacent fringes corresponds to interplanar distances characteristic of TiN crystallographic planes, confirming the presence of well-ordered atomic arrangements. The continuity and regularity of these fringes suggest a relatively low density of structural defects such as dislocations, stacking faults, or twin boundaries. This observation is particularly significant, as it demonstrates that despite the presence of some local disorder—as inferred from Raman spectroscopy—the crystalline regions maintain a high level of atomic order. Such a combination of ordered and disordered domains is expected to contribute to the unique physical and chemical properties of the synthesized material.

Fast Fourier transform (FFT) analysis was carried out on selected regions of the TEM micrographs, as shown in Figure 2d, to obtain additional structural information at the atomic scale. This analytical technique enabled the identification and measurement of interplanar lattice distances within the crystalline domains of the synthesized material. The FFT patterns revealed distinct diffraction spots corresponding to periodic spacings of 0.177 nm and 0.353 nm. These measured distances are consistent with the interplanar spacings associated with the (104) and (101) crystallographic planes of titanium nitride, respectively. The clear and well-defined nature of the diffraction maxima supports the presence of extended crystalline regions within the sample, further confirming the high degree of structural order achieved under the applied synthesis conditions.

The symmetry and spatial arrangement of the diffraction spots observed in the FFT patterns suggest that the crystalline domains exhibit a uniform orientation and minimal distortion across the analyzed areas. This level of structural coherence implies a low density of long-range lattice defects such as grain boundaries or significant dislocations, which would otherwise lead to broader or more diffuse scattering features. Therefore, the FFT results corroborate the conclusions drawn from both XRD and Raman spectroscopy regarding the coexistence of amorphous and crystalline phases, with the latter displaying a relatively high degree of internal structural organization.

To further quantify the crystallinity and assess the periodicity of the lattice structure, intensity profile analysis was performed along selected lattice fringes visible in the HRTEM images (Figure 2e). This line-profile analysis allowed for the precise determination of fringe spacing by measuring the distance between consecutive bright and dark contrast regions, which correspond to atomic planes within the crystal lattice. The resulting measurements yielded an average interplanar spacing of 3.561 Å. This value is in close agreement with the theoretical d-spacing of 3.548 Å calculated for the (101) plane of titanium nitride based on its cubic crystal structure. The small deviation between the experimental and theoretical values falls within the expected range of measurement uncertainty and does not indicate any significant structural distortion or compositional variation at this level of resolution.

Collectively, these TEM and FFT analyses provide comprehensive evidence for the coexistence of well-ordered crystalline domains and disordered regions within the synthesized material, highlighting its complex and hierarchical microstructure. This dual-phase structure is likely to play a crucial role in determining the material's functional properties, including its electronic, thermal, and mechanical behavior, and may offer new opportunities for tailoring its performance in advanced applications.

4. Conclusions

The synthesis of TiNCl using the flash Joule heating (FJH) method has demonstrated an innovative and efficient approach for producing two-dimensional nanomaterials with promising structural and chemical properties. The single-step process involved applying

high-intensity electrical pulses to $TiCl_4$ under an inert nitrogen atmosphere, resulting in a structure composed of crystalline TiNCl domains. Combined analysis of XRD, Raman spectroscopy, and DRIFT confirmed the formation of Ti–N bonds and the absence of undesired phases, such as titanium oxides, evidencing the purity of the synthesized material. Additionally, TEM images revealed the characteristic lamellar morphology of 2D materials, while FFT diffraction patterns corroborated local crystalline order in the analyzed regions. These results highlight the effectiveness of FJH in producing halogenated MXene-like materials with controlled microstructure and composition, overcoming limitations associated with conventional methods.

FJH presents a significant alternative to traditional synthesis routes, such as acid etching or chemical vapor deposition (CVD), which frequently require multiple steps, hazardous reagents, or high energy costs. The proposed approach eliminates the need for toxic solvents and drastically reduces reaction time, typically completed within minutes, in contrast to conventional processes that may take hours or days. Furthermore, the use of $TiCl_4$ as a single precursor, combined with an inert nitrogen environment, prevents the formation of undesired by-products, such as TiO_2, which would compromise the conductivity and stability of the material. This operational simplicity, combined with scalability capability, positions FJH as a viable strategy for industrial production of MXenes, especially those with complex compositions, such as halogenated variants.

The coexistence of crystalline and amorphous phases in the obtained material is a critical aspect for its functional properties. Well-defined crystalline domains contribute to metallic conductivity and thermal stability. This dual-phase architecture also favors modulation of electronic and mechanical characteristics, enabling fine-tuning for specific applications. For example, the presence of defects or distortions in the crystalline lattice, observed through deviations in diffraction peaks and hybrid vibrational modes in the Raman spectrum, suggests the possibility of band engineering to optimize performance in optoelectronic devices or photocatalysts.

The environmental and economic implications of FJH are equally relevant. By avoiding the use of hazardous reagents and reducing energy consumption, the method aligns with green chemistry principles, mitigating ecological impacts associated with nanomaterial production. Its rapid and continuous nature also facilitates integration into automated manufacturing lines, potentially reducing production costs and accelerating commercial adoption. Future studies should explore optimization of synthesis conditions for greater control over layer thickness and the proportion between crystalline and amorphous phases, as well as surface functionalization for specific applications, such as electrochemical sensors or energy storage systems.

Author Contributions: Conceptualization, E.P.S., A.O.N. and R.F.B.d.S.; methodology, G.A.S. and M.A.; formal analysis, R.F.B.d.S.; investigation, G.A.S. and R.F.B.d.S.; resources, A.O.N.; data curation, A.O.N.; writing—original draft preparation, A.O.N. and R.F.B.d.S.; writing—review and editing, E.F.U.d.C.; supervision, R.F.B.d.S.; funding acquisition, A.O.N. All authors have read and agreed to the published version of the manuscript.

Funding: This research was funded by CAPES, CNPq (350514/2023-2, 302709/2020-7).

Data Availability Statement: Data are contained within the article. Further inquiries can be directed to the corresponding author.

Acknowledgments: Rodrigo Fernando Brambilla de Souza extends special gratitude to the execution team for the Brazilian Multipurpose Reactor (RMB/CNEN) Project.

Conflicts of Interest: The authors declare no conflicts of interest.

References

1. Xu, J.; Peng, T.; Qin, X.; Zhang, Q.; Liu, T.; Dai, W.; Chen, B.; Yu, H.; Shi, S. Recent Advances in 2d Mxenes: Preparation, Intercalation and Applications in Flexible Devices. *J. Mater. Chem. A* **2021**, *9*, 14147–14171. [CrossRef]
2. Sharbirin, A.S.; Roy, S.; Tran, T.T.; Akhtar, S.; Singh, J.; Duong, D.L.; Kim, J. Light-Emitting Ti2N (Mxene) Quantum Dots: Synthesis, Characterization and Theoretical Calculations. *J. Mater. Chem. C* **2022**, *10*, 6508–6514. [CrossRef]
3. Fan, J.; Wang, H.; Sun, W.; Duan, H.; Jiang, J. Recent Developments and Perspectives of Ti-Based Transition Metal Carbides/Nitrides for Photocatalytic Applications: A Critical Review. *Mater. Today* **2024**, *76*, 110–135. [CrossRef]
4. Zhang, T.; Shuck, C.E.; Shevchuk, K.; Anayee, M.; Gogotsi, Y. Synthesis of Three Families of Titanium Carbonitride MXenes. *J. Am. Chem. Soc.* **2023**, *145*, 22374–22383. [CrossRef]
5. Urbankowski, P.; Anasori, B.; Makaryan, T.; Er, D.; Kota, S.; Walsh, P.L.; Zhao, M.; Shenoy, V.B.; Barsoum, M.W.; Gogotsi, Y. Synthesis of Two-Dimensional Titanium Nitride Ti4N3 (Mxene). *Nanoscale* **2016**, *8*, 11385–11391. [CrossRef]
6. Kruger, D.D.; García, H.; Primo, A. Molten Salt Derived Mxenes: Synthesis and Applications. *Adv. Sci.* **2024**, *11*, 2307106. [CrossRef] [PubMed]
7. Tanaka, M.; Kataoka, N.; Matsumoto, R.; Inumaru, K.; Takano, Y.; Yokoya, T. Synthetic Route of Layered Titanium Nitride Chloride TiNCl Using Sodium Amide. *ACS Omega* **2022**, *7*, 6375–6380. [CrossRef] [PubMed]
8. Yue, F.; Xiang, M.; Zheng, J.; Zhu, J.; Wei, J.; Yang, P.; Shi, H.; Dong, Q.; Ding, W.; Chen, C.; et al. One-Step Gas-Phase Syntheses of Few-Layered Single-Phase Ti_2NCl_2 and Ti_2CCl_2 Mxenes with High Stabilities. *Nat. Commun.* **2024**, *15*, 10334. [CrossRef]
9. Wang, D.; Zhou, C.; Filatov, A.S.; Cho, W.; Lagunas, F.; Wang, M.; Vaikuntanathan, S.; Liu, C.; Klie, R.F.; Talapin, D.V. Direct Synthesis and Chemical Vapor Deposition of 2D Carbide and Nitride Mxenes. *Science* **2023**, *379*, 1242–1247. [CrossRef] [PubMed]
10. Liang, Y.; Dai, Y.; Ma, Y.; Ju, L.; Wei, W.; Huang, B. Novel Titanium Nitride Halide TiNX (X = F, Cl, Br) Monolayers: Potential Materials for Highly Efficient Excitonic Solar Cells. *J. Mater. Chem. A* **2018**, *6*, 2073–2080. [CrossRef]
11. Zhao, S.; Dong, C.; Wang, X.; Tang, Y.; Huang, F. A Dual-Functional Titanium Nitride Chloride Layered Matrix with Facile Lithium-Ion Diffusion Path and Decoupled Electron Transport as High-Capacity Anodes. *Adv. Funct. Mater.* **2022**, *32*, 2112074. [CrossRef]
12. Chen, W.; Li, J.T.; Wang, Z.; Algozeeb, W.A.; Luong, D.X.; Kittrell, C.; McHugh, E.A.; Advincula, P.A.; Wyss, K.M.; Beckham, J.L.; et al. Ultrafast and Controllable Phase Evolution by Flash Joule Heating. *ACS Nano* **2021**, *15*, 11158–11167. [CrossRef] [PubMed]
13. Li, J.; Wang, C.; Chen, X.; Zhang, Y.; Zhang, Y.; Fan, K.; Zong, L.; Wang, L. Flash Synthesis of Ultrafine and Active NiRu Alloy Nanoparticles on N-Rich Carbon Nanotubes via Joule Heating for Efficient Hydrogen and Oxygen Evolution Reaction. *J. Alloys Compd.* **2023**, *959*, 170571. [CrossRef]
14. Billinge, S.J.L.; Kanatzidis, M.G. Beyond Crystallography: The Study of Disorder, Nanocrystallinity and Crystallographically Challenged Materials with Pair Distribution Functions. *Chem. Commun.* **2004**, 749–760. [CrossRef]
15. Ansari, S.A.; Khan, N.A.; Hasan, Z.; Shaikh, A.A.; Ferdousi, F.K.; Barai, H.R.; Lopa, N.S.; Rahman, M.M. Electrochemical Synthesis of Titanium Nitride Nanoparticles Onto Titanium Foil for Electrochemical Supercapacitors with Ultrafast Charge/Discharge. *Sustain. Energy Fuels* **2020**, *4*, 2480–2490. [CrossRef]
16. Xie, B.; Liu, J. Lattice Distortions, moir\'e Phonons, and Relaxed Electronic Band Structures in Magic-Angle Twisted Bilayer Graphene. *Phys. Rev. B* **2023**, *108*, 094115. [CrossRef]
17. Djire, A.; Zhang, H.; Liu, J.; Miller, E.M.; Neale, N.R. Electrocatalytic and Optoelectronic Characteristics of the Two-Dimensional Titanium Nitride Ti4N3Tx MXene. *ACS Appl. Mater. Interfaces* **2019**, *11*, 11812–11823. [CrossRef]
18. Cheng, P.; Ye, T.; Zeng, H.; Ding, J. Raman Spectra Investigation on the Pressure-Induced Phase Transition in Titanium Nitride (TiN). *AIP Adv.* **2020**, *10*, 045110. [CrossRef]
19. Subramanian, B.; Muraleedharan, C.V.; Ananthakumar, R.; Jayachandran, M. A Comparative Study of Titanium Nitride (TiN), Titanium Oxy Nitride (TiON) and Titanium Aluminum Nitride (TiAlN), as Surface Coatings for Bio Implants. *Surf. Coat. Technol.* **2011**, *205*, 5014–5020. [CrossRef]
20. Chen, C.C.; Liang, N.T.; Tse, W.S.; Chen, I.Y.; Duh, J.-G. Raman Spectra of Titanium Nitride Thin Films. *J. Chin. J. Phys.* **1994**, *32*, 205–210.
21. Judek, J.; Wróbel, P.; Michałowski, P.P.; Ożga, M.; Witkowski, B.; Seweryn, A.; Struzik, M.; Jastrzębski, C.; Zberecki, K. Titanium Nitride as a Plasmonic Material from Near-Ultraviolet to Very-Long-Wavelength Infrared Range. *Materials* **2021**, *14*, 7095. [CrossRef] [PubMed]

22. Kim, S.-J.; Kim, B.-H.; Woo, H.-G.; Kim, S.-K.; Kim, D.-H. Thermal Decomposition of Tetrakis(ethylmethylamido) Titanium for Chemical Vapor Deposition of Titanium Nitride. *Bull. Korean Chem. Soc.* **2006**, *27*, 219–223. [CrossRef]
23. Morozov, I.G.; Belousova, O.V.; Belyakov, O.A.; Parkin, I.P.; Sathasivam, S.; Kuznetcov, M.V. Titanium Nitride Room-Temperature Ferromagnetic Nanoparticles. *J. Alloys Compd.* **2016**, *675*, 266–276. [CrossRef]